Comparison of Cyclic Deformation Behavior between Copper Bicrystals and Their Component Crystals

Z.F. ZHANG and Z.G. WANG

In this article, the cyclic deformation behavior of a combined copper bicrystal (CB), a naturally grown copper bicrystal (RB), and their component crystals (G1 and G2) was investigated under total strain amplitude control at room temperature in air. The bicrystal CB without grain boundary (GB) was prepared by joining the two single slip–oriented component crystals G1 and G2 in the gage. The results showed that the cyclic hardening rates and the axial stresses increased, in order, in the component crystal G2, the bicrystal CB, the bicrystal RB, and the component crystal G1. The cyclic stress-strain curves (CSSCs) of the component crystals G1 and G2 and the bicrystal CB exhibited a plateau behavior under the selected strain range. However, the cyclic saturation stress of the bicrystal RB increased with strain amplitude and did not show a plateau in its CSSC. Surface observations of the copper bicrystals and the component crystals revealed that the cyclic plastic strains were carried by the primary slip (B4) within the component crystals in the bicrystal CB and its component crystal G1 and G2. However, an additional slip (A3) within the component crystal G2 was observed in the vicinity of the GB in the bicrystal RB. The width of the additional slip region increased with strain amplitude and varied in the range from 265 to 650 μm. In order to compare the CSSCs of the copper bicrystals and their component crystals, an "orientation factor" for the copper bicrystal was introduced and the effect of the GB on the bicrystal RB is quantified during cyclic deformation.

I. INTRODUCTION

It is well known that copper, single crystal oriented for single slip, exhibits a plateau region over a resolved shear plastic strain range from 6.0×10^{-5} to 7.5×10^{-3} in cyclic stress-strain curve (CSSC).[11] Most investigators[2,3] have found that the plateau saturation resolved shear stress at room temperature lies in the range from 28 to 30 MPa, nearly independent of the crystal orientations when the crystal orientation orients for single slip. Meanwhile, the cyclic deformation behavior of copper polycrystals was also investigated extensively. It was found that the CSSCs of some copper polycrystals also exhibited a plateau feature over certain strain ranges.[4–7] However, Mughrabi[8] and Lukas and Kunz[9] suggested that there should not be any plateau region in the CSSCs of copper polycrystals.

In order to compare the deformation features between monocrystals and polycrystals, the effects of both grain boundaries (GBs) and crystal orientations should be considered. Each grain in a polycrystal has its own stress-strain characteristic, whereas the stress-strain response of the whole polycrystal is not a simple "average" over all the grains.[10] The reason is that the grains in a polycrystal do not deform independently. The strain compatibility requirement leads to the operation of secondary slip in the vicinity of GBs.[11,12] To clarify the difference in plastic deformation between monocrystals and polycrystals, the bicrystal is often regarded as an important model material for revealing the effects of GBs and component crystals. However, most of the studies on bicrystals were performed under monotonic loading conditions.[12–17] Only very limited work on

the fatigue behavior of bicrystals such as α-β brass,[18] aluminum,[19] α-Ti,[20] an Fe-Si alloy[21] and copper bicrystals,[22–26] can be found. Recent studies[23,24] on copper bicrystals with a parallel GB revealed that the saturation stresses can be increased by the GB. However, the component crystal orientations have a decisive effect on the CSSC of the bicrystal with a perpendicular GB.[22,25,26] In order to further study the cyclic deformation behavior of copper bicrystals, the effects of both component crystals and GB on the fatigue behavior of copper bicrystals will be investigated separately in this article.

II. EXPERIMENTAL PROCEDURE

A bicrystal plate measuring $200 \times 50 \times 10$ mm^3 was grown from oxygen-free high-conductivity copper of 99.999 pct purity, by the Bridgman method, in a horizontal furnace, and the GB was parallel to the growth direction. In order to compare the cyclic deformation behavior of bicrystals with their component crystals, three kinds of fatigue specimens were made from the grown bicrystal plate. They are (1) the fatigue specimen of a naturally grown copper bicrystal (RB) with a GB parallel to the stress axis (Figure 1(a)); (2) the fatigue specimens of two component crystals, G1 and G2, as shown in Figure 1(b); and (3) the fatigue specimen of a "combined" bicrystal (CB) by sticking the component crystals G1 and G2 together at the grip parts, as indicated in Figure 1(c). All the fatigue specimens are 3-mm thick. Using these specially designed fatigue specimens, the effects of the component crystals and the GB on the fatigue behavior of the bicrystal RB under cyclic loading can be separately elucidated.

By using the X-ray Laue back-reflection method, the orientations of the two component crystals were determined. The component crystal orientations in the bicrystals RB and CB are shown in Figure 2(a); it is clear that both the com-

Z.F. ZHANG, Postdoctoral Student, and Z.G. WANG, Professor, are with the Institute of Metal Research, Chinese Academy of Science, Shenyang 110015, People's Republic of China.
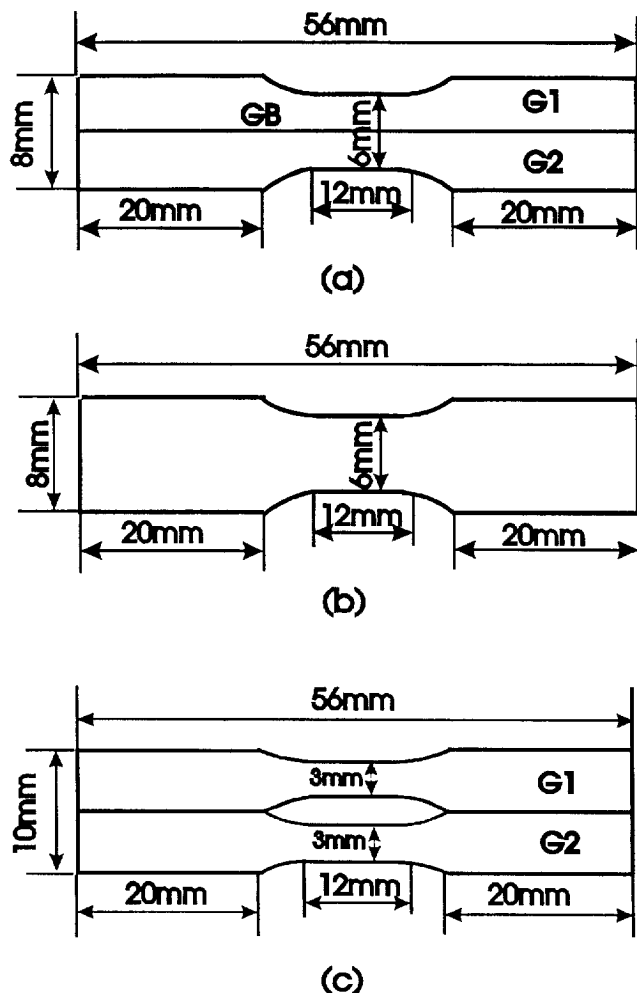
Fig. 1—Fatigue specimens of the copper bicrystals and their component crystals. (a) A bicrystal RB, (b) the component crystal G1 or G2, and (c) a bicrystal CB.

ponent crystals G1 and G2 orient for single slip. In particular, their Schmid factors (Ω_{G1} and Ω_{G2}) have a great difference and are equal to 0.35 and 0.47, respectively. The crystallographic relations of the primary slip plane and the GB in the bicrystal RB are shown in Figure 2(b). Before cyclic deformation, all the fatigue specimens were electropolished carefully for surface observation. Cyclic push-pull tests were performed on a Shimadzu servohydraulic testing machine, under constant total strain amplitude control, at room temperature in air. A triangle wave with a frequency of 0.2 Hz was used. The selected total strain amplitudes were 0.10, 0.15, 0.20, 0.25, and 0.30 pct and are approximately in the range of the plateau region in the CSSC of a copper monocrystal.[11] Peak loads in tension and compression and hysteresis loops were automatically recorded by computer. After cyclic saturation, these specimens were observed by optical microscopy (OM), especially in the vicinity of the GB in the bicrystal RB.

III. RESULTS

A. Cyclic Hardening Behavior

In Figures 3(a) and (b), the cyclic hardening curves of the copper bicrystals and the component crystals, cycled at
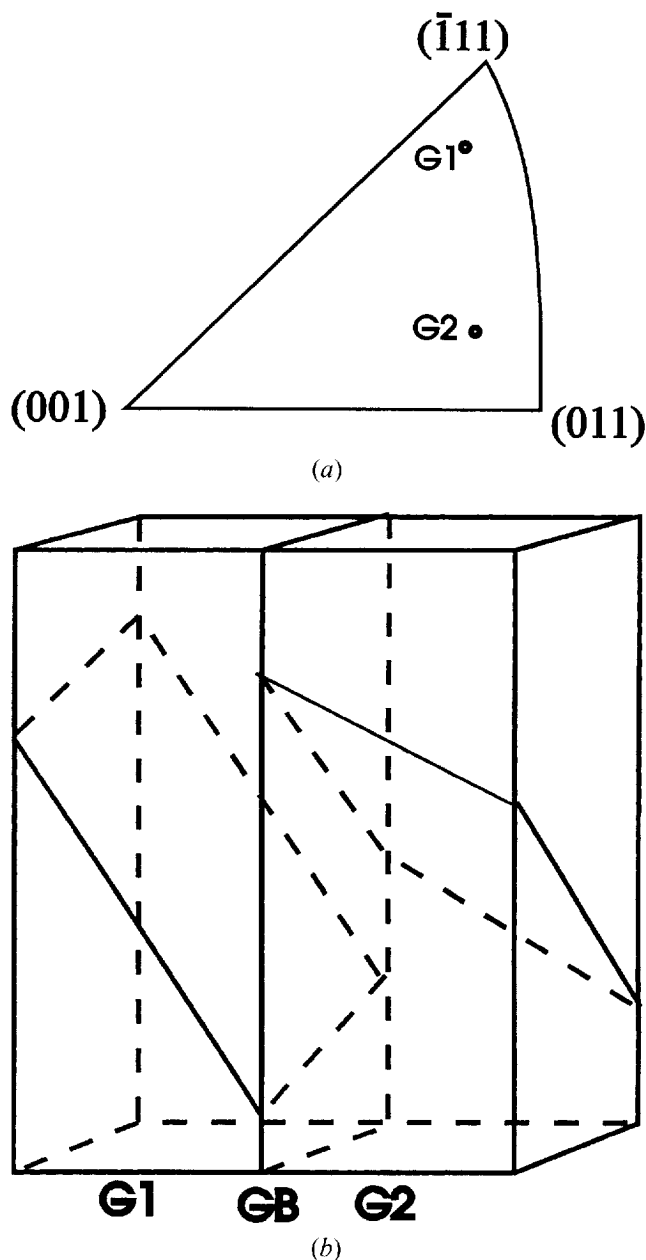

Fig. 2—The component crystal orientations and the crystallographic relations of the copper bicrystals. (a) The orientations of the component crystals in the stereographic triangle and (b) the crystallographic relations of the primary slip planes and GB in the bicrystal RB.

the strain amplitudes of 0.15 and 0.25 pct, are shown. It can be found that the cyclic hardening rates and the axial cyclic stress increase, in order, in the component crystal G2, the bicrystal CB, the bicrystal RB, and the component crystal G1 under the same strain amplitude. With further cyclic deformation, all those specimens exhibited a cyclic saturation behavior at all the strain amplitudes. During cyclic hardening, the plastic strains of the component crystals and the bicrystals decreased continuously until cyclic saturation occurred, because the specimens were cycled under constant total strain amplitude control, as indicated in Figures 4(a) and (b). The cyclic plastic strains of the component crystals show a great difference at the same strain amplitude due to the difference in their orientations. It is,
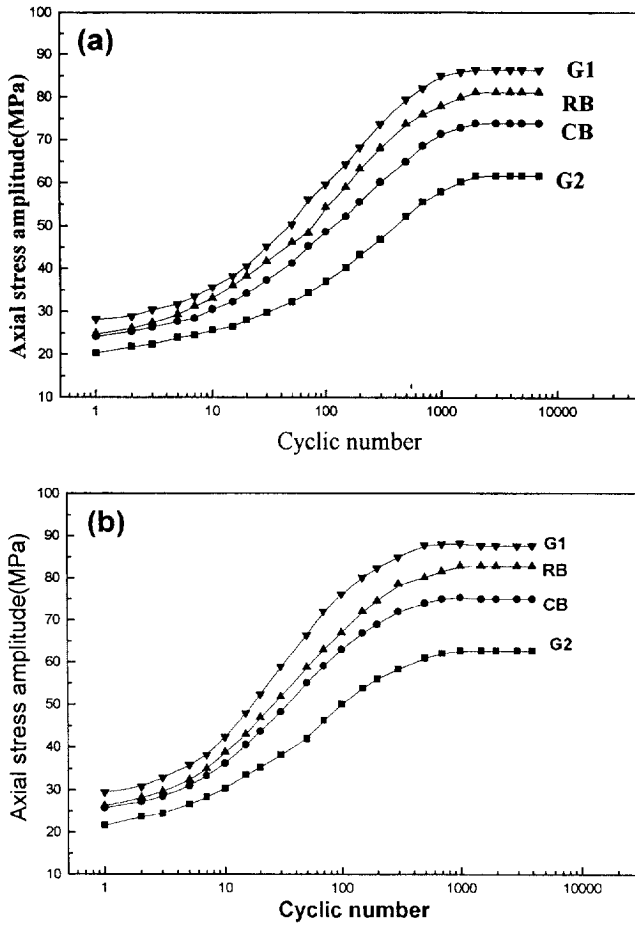
Fig. 3—Cyclic hardening curves of the bicrystals and the component crystals cycled at the strain amplitudes of 0.15 and 0.25 pct: (*a*) ε_a = 0.15 pct and (*b*) ε_a = 0.25 pct.

therefore, expected that the bicrystal RB will have a great stress-strain incompatibility, especially under cyclic loading. However, the saturation plastic strains of both the bicrystals nearly reached the same value and are between those of the component crystals.

B. *Cyclic Stress-Strain Curves*

The cyclic saturation axial stress (σ_{as}), resolved shear stress (τ_{as}), axial plastic strain amplitude (ε_{pl}), and plastic resolved shear strain amplitude (γ_{pl}) of the bicrystals and the component crystals are listed in Table I. Here, the saturation resolved shear stresses and the plastic resolved shear strains of the component crystals are calculated by using their Schmid factors (Ω_{G1} and Ω_{G2}), *i.e.*,

$$\tau_{as}^{G1} = \sigma_{as}^{G1}\Omega_{G1} \qquad [1]$$
$$\gamma_{pl}^{G1} = \varepsilon_{pl}^{G1}/\Omega_{G1}$$

$$\tau_{as}^{G2} = \sigma_{as}^{G2}\Omega_{G2} \qquad [2]$$
$$\gamma_{pl}^{G2} = \varepsilon_{pl}^{G2}/\Omega_{G2}$$

For the bicrystals, their saturation resolved shear stresses and resolved shear strains can be calculated by introducing an "orientation factor" (Ω_B) of the bicrystal, as discussed in the following section. For the combined bicrystal,
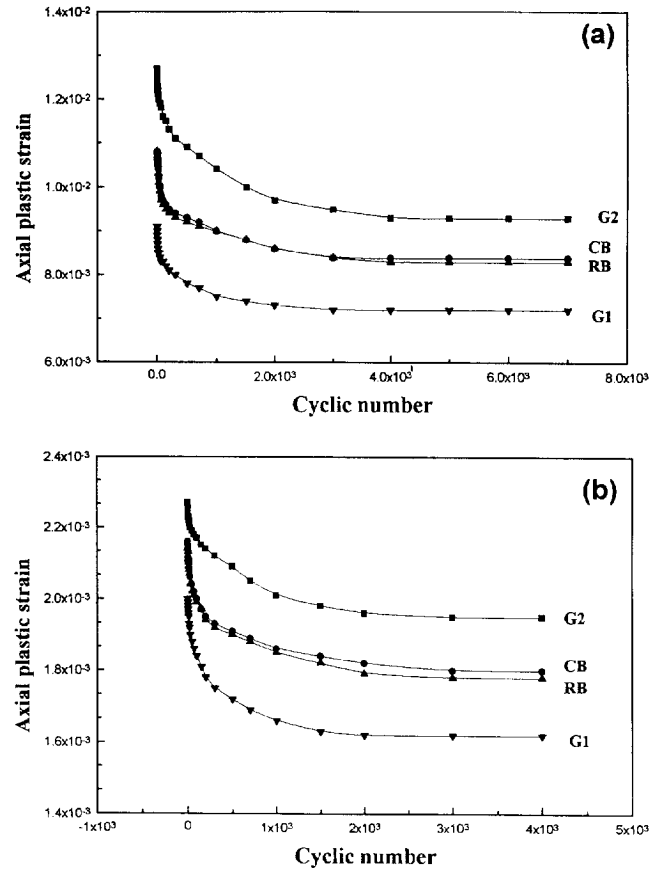

Fig. 4—The curves of axial plastic strain *vs* cyclic number of the bicrystals and the component crystals cycled at the strain amplitudes of 0.15 and 0.25 pct: (*a*) ε_a = 0.15 pct and (*b*) ε_a = 0.25 pct.

Table I. The Cyclic Saturation Stresses and Plastic Strains of the Bicrystals and Their Component Crystals

	ε_a (10^{-3})	ε_{pl} (10^{-3})	σ_{as} (MPa)	γ_{pl} (10^{-3})	τ_{as} (MPa)
G1	1.0	0.25	86.5	0.71	30.3
	1.5	0.72	86.8	2.06	30.4
	2.0	1.12	87.2	3.20	30.5
	2.5	1.73	87.7	4.94	30.7
	3.0	2.12	88.0	6.06	30.8
G2	1.0	0.45	61.2	0.96	28.8
	1.5	0.91	61.7	1.94	29.0
	2.0	1.45	62.1	3.09	29.2
	2.5	1.92	62.4	4.08	29.3
	3.0	2.44	62.8	5.18	29.5
CB	1.0	0.36	73.6	0.90	29.4
	1.5	0.84	74.0	2.10	29.6
	2.0	1.34	74.5	3.35	29.8
	2.5	1.82	74.8	4.55	29.9
	3.0	2.23	75.0	5.58	30.0
RB	1.0	0.35	78.5	0.88	31.4
	1.5	0.83	80.2	2.08	32.1
	2.0	1.32	81.8	3.30	32.7
	2.5	1.81	83.5	4.53	33.3
	3.0	2.20	84.8	5.50	34.0

$$\tau_{as}^{CB} = \sigma_{as}^{CB}\Omega_B \qquad [3]$$
$$\gamma_{pl}^{CB} = \varepsilon_{pl}^{CB}/\Omega_B$$

And, for the naturally grown bicrystal,

(a)

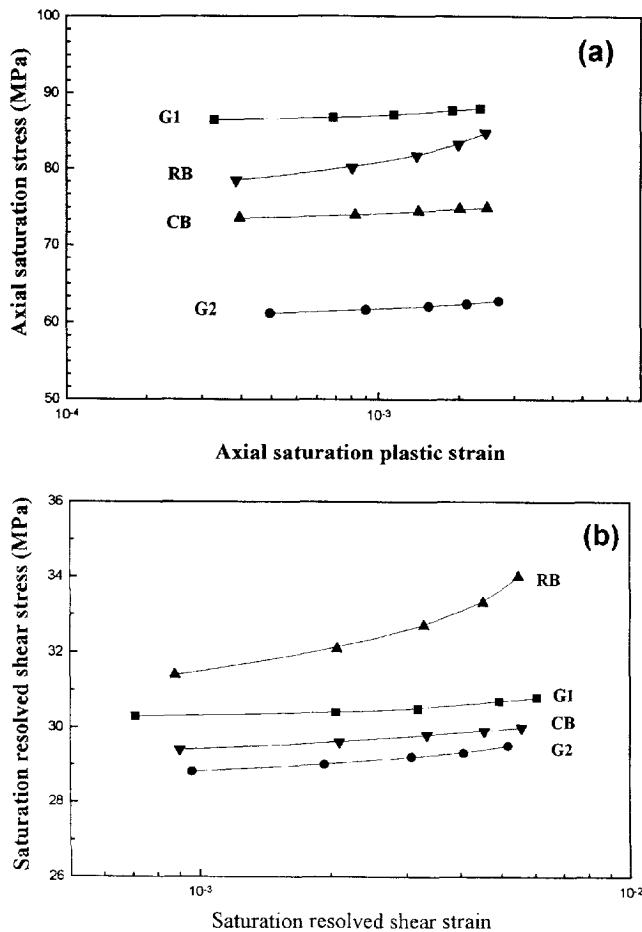Axial saturation plastic strain

(b)

Saturation resolved shear strain

Fig. 5—The CSSCs of the bicrystals and the component crystals. (a) The curves of axial saturation stress vs axial saturation plastic strain and (b) the curves of saturation resolved shear stress vs saturation plastic resolved shear strain.

$$\tau_{as}^{RB} = \sigma_{as}^{RB}\Omega_B$$

$$\gamma_{pl}^{RB} = \varepsilon_{pl}^{RB}/\Omega_B$$ [4]

In Figure 5(a), the curves of axial saturation stress vs axial saturation plastic strain carried by the component crystals and the bicrystals are shown. It can be seen that the saturation stresses increase, in order, in the component crystal G2, the bicrystal CB, the bicrystal RB, and the component crystal G1. Similar to the cyclic deformation behavior of the copper single crystal oriented for single slip,[1,2,3] the CSSCs of the component crystals as well as the bicrystal CB also show a plateau behavior within the measured strain range. The plateau saturation stress of the bicrystal CB is basically equal to the mean value of those of the component crystals. However, the axial saturation stress of the bicrystal RB is obviously higher than that of the bicrystal CB and increases with strain amplitude.

The curves of the saturation resolved shear stress vs saturation plastic resolved shear strain carried by the component crystals and the bicrystals are shown in Figure 5(b). The plateau saturation resolved shear stresses of the component crystals and the bicrystal CB nearly maintain the same value in the range from 29 to 31 MPa, basically consistent with the results of the copper single crystals oriented for single slip.[1,2,3] But the bicrystal RB does not display a plateau in its CSSC and shows a higher saturation stress
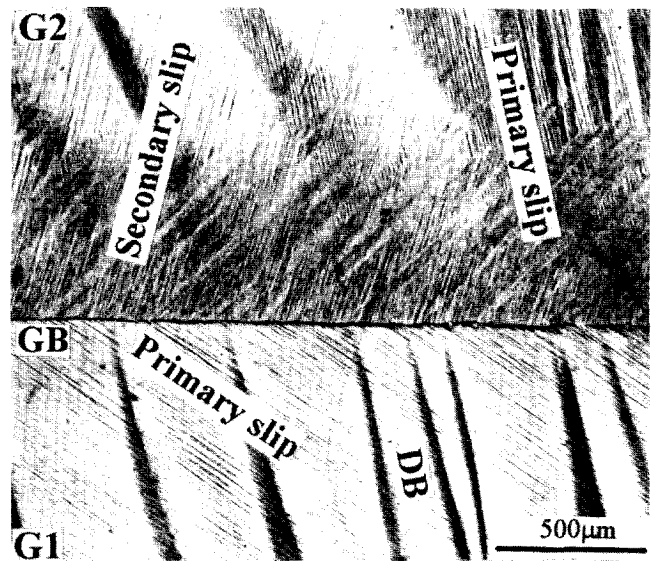

Fig. 6—The slip morphology of the bicrystal RB cycled at the strain amplitude of 0.30 pct for 3000 cycles.

than that of the bicrystal CB. This behavior of the bicrystal RB should be attributed to the existence of the GB.

C. Surface Observation on the Component Crystals and the Bicrystals

Surface observation by OM revealed that only the primary slip system B4 (111)[$\bar{1}$01] was activated in the component crystals and in the bicrystal CB under all the selected strain amplitudes. This means that the cyclic plastic strains of the component crystals and the bicrystal CB are carried by the primary slip system (B4). In contrast, a secondary slip system, A3 ($\bar{1}$11)[101], was activated in the vicinity of the GB within the component crystal G2 in the bicrystal RB, as shown in Figure 6. It is clear that there is no secondary slip within the component crystal G1, except for some deformation bands (DBs). Meanwhile, the range of the secondary slip region within the component crystal G2 increases with increasing strain amplitude, as shown in Figures 7(a) and (b). The mean width (D_{GB}) and volume fraction (V_{GB}) of the secondary slip region in the vicinity of the GB are measured and listed in Table II. With increasing strain amplitude, the interaction of primary slip (B4) with the secondary slip (A3) becomes more serious. The primary slip lines are regularly modulated by the secondary lines and no other slip systems are involved, as is more clearly shown in Figures 8(a) and (b), taken using a differential interference contrast technique. The primary slip lines and secondary slip lines alternately emerge, creating a cross weaved–like structure, and a GB-affected zone (GBAZ) formed. This phenomenon should be associated with the stress-strain incompatibility at the GB. The region in the vicinity of the GB often exhibits stress-strain incompatibility, especially under cyclic loading. The concept of the GBAZ was introduced by Rey and Zaoui.[14,15] The operation of multiple slip was also observed in copper bicrystals under cyclic loading.[22–26] However, such a strong and regular secondary slip region (Figures 6 through 8) was not observed before. By analyzing the slip traces, the operated slip systems were determined to be B4 and A3 (sec-
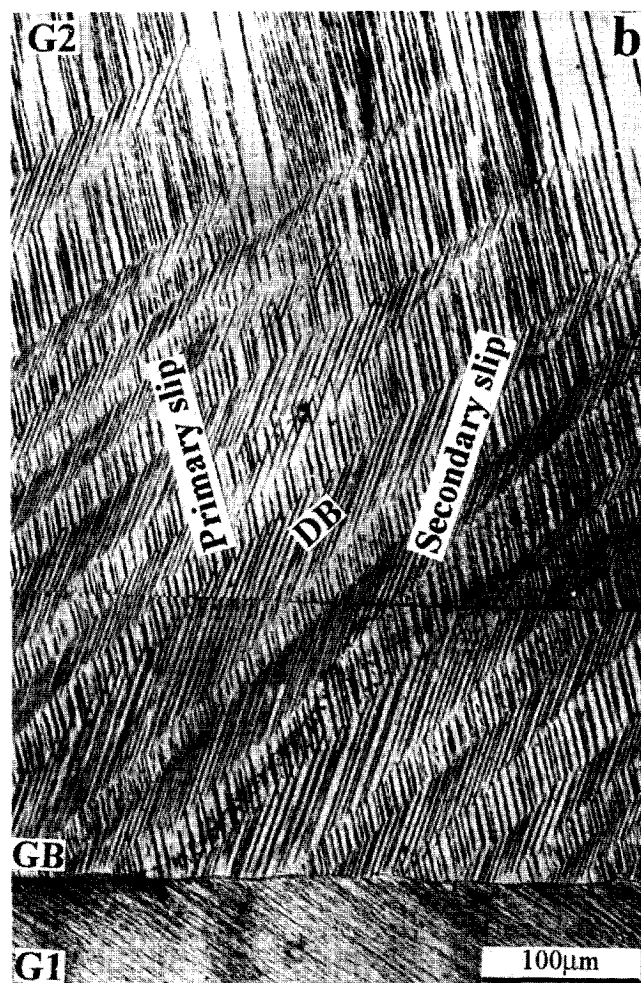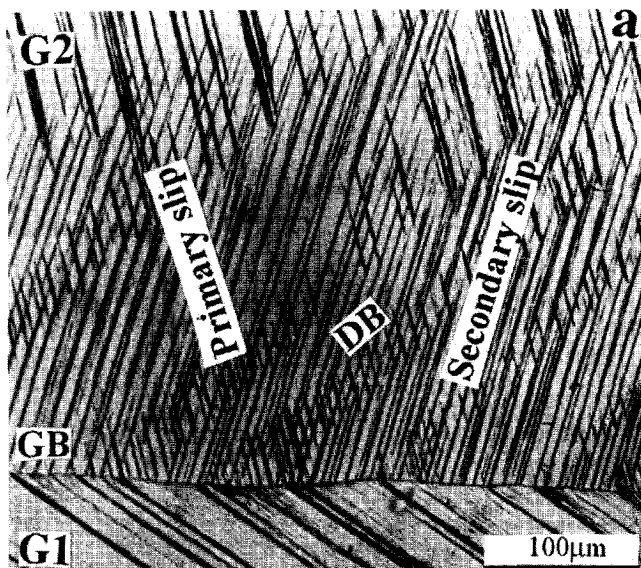
Fig. 7—The slip patterns in the vicinity of GB in the bicrystal RB cycled at different strain amplitudes: (a) ε_a = 0.15 pct for 7000 cycles and (b) ε_a = 0.25 pct for 4000 cycles.

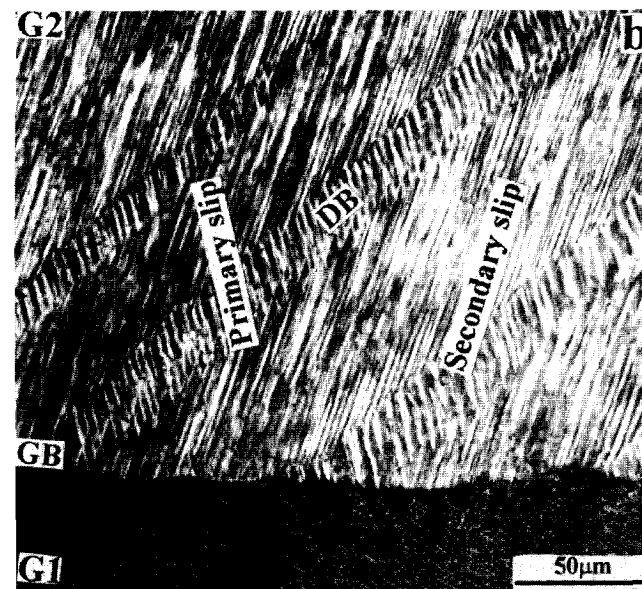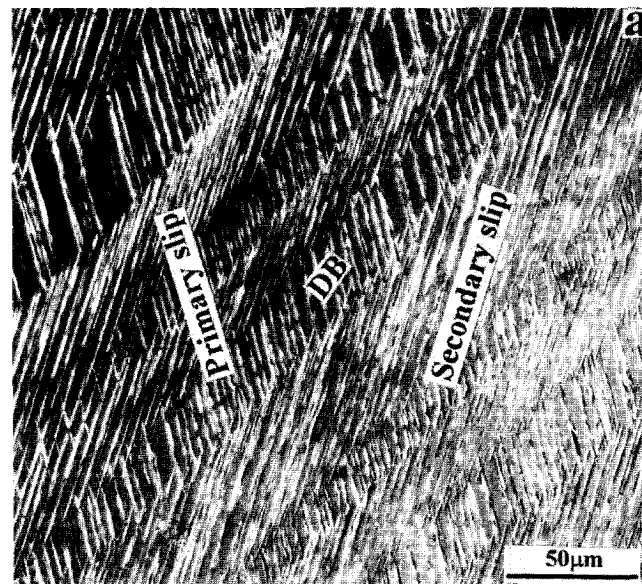| Strain Amplitude	0.1 Pct	0.15 Pct	0.2 Pct	0.25 Pct	0.3 Pct
D_{GB} (μm)	265	360	440	540	650
V_{GB} (pct)	4.4	6.0	7.3	9.0	10.5

Fig. 8—The interaction of the primary slip lined with the secondary slip lines in the bicrystal RB cycled at the strain amplitude of 0.30 pct for 3000 cycles: (b) in the vicinity of GB and (a) apart from the GB.

plastic incompatibility in the vicinity of the GB also became serious as the strain amplitude was increased, and a higher stress concentration near the GB may exist, owing to the secondary slip operation.

IV. DISCUSSION

A. Orientation Factor for Copper Bicrystals

The Schmid factor Ω is widely used to calculate the resolved shear stress of single crystals from the imposed axial

ondary slip) in the bicrystal RB. In addition, it can be seen that the secondary slip region does not spread throughout the whole crystal, and the range of the GBAZ increases with increasing strain amplitude. It is indicated that the
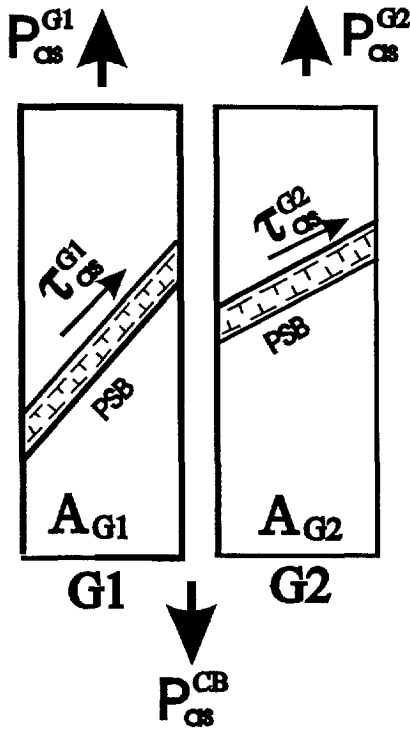
Fig. 9—The diagrammatic sketch of stress distribution in the combined bicrystal CB.

stress. For a polycrystal, the Taylor factor ($M = 3.06$) or the Saches factor ($M = 2.24$) is often employed.[6,7,10,11,14] However, the orientation factor of a bicrystal was seldom discussed.

For a bicrystal specimen with two individual single crystals (G1 and G2) combined in parallel, as shown in Figure 9, the two component crystals will deform independently owing to the absence of a GB. As the bicrystal specimen CB was cyclically saturated, according to the force balance, we have

$$P_{as}^{CB} = P_{as}^{G1} + P_{as}^{G2} \qquad [5]$$

and

$$\sigma_{as}^{CB} A_{CB} = \sigma_{as}^{G1} A_{G1} + \sigma_{as}^{G2} A_{G2} \qquad [6]$$

where P_{as}^{CB}, P_{as}^{G1}, and P_{as}^{G2} are the loads applied to the cyclically saturated bicrystal CB and the component crystals, G1 and G2, respectively; σ_{as}^{CB}, σ_{as}^{G1}, and σ_{as}^{G2} are the mean axial saturation stresses applied to the bicrystal CB and the component crystals, G1 and G2, respectively; Ω_B, Ω_{G1}, and Ω_{G2} are the orientation factors of the bicrystal CB and the component crystals, G1 and G2, respectively; and A_{CB}, A_{G1}, and A_{G2} are the areas of the bicrystal CB and the component crystals, G1 and G2, respectively. Substituting the saturation resolved shear stresses (τ_{as}^{G1}, τ_{as}^{G2}, and τ_{as}^{CB}) and Schmid factors (Ω_{G1}, Ω_{G2}, and Ω_B) of the two component crystals and the bicrystal CB, we can obtain

$$\frac{\tau_{as}^{CB}}{\Omega_B} A_{CB} = \frac{\tau_{as}^{G1}}{\Omega_{G1}} A_{G1} + \frac{\tau_{as}^{G2}}{\Omega_{G2}} A_{G2} \qquad [7]$$

It is well known that the saturation resolved shear stress τ_{as}^{PSB} of the copper single crystal oriented for single slip

maintained a constant value in the range from 28 to 30 MPa in region B of its CSSC and was independent of crystal orientations.[1,2,3] Because there is no GB in the bicrystal CB, it can be considered that the saturation resolved shear stress of the bicrystal CB should be equal to that of the component crystals, as listed in Table I, *i.e.*,

$$\tau_{as}^{CB} = \tau_{as}^{G1} = \tau_{as}^{G2} = \tau_{as}^{PSB} \qquad [8]$$

Substituting Eq. [8] into Eq. [7], we can obtain

$$\frac{1}{\Omega_B} = \frac{V_{G1}}{\Omega_{G1}} + \frac{V_{G2}}{\Omega_{G2}} \qquad [9]$$

Where V_{G1} and V_{G2} are the volume fraction of the component crystals G1 and G2 in a bicrystal, respectively; *i.e.*,

$$V_{G1} = \frac{A_{G1}}{A_{CB}}$$
$$V_{G2} = \frac{A_{G2}}{A_{CB}} \qquad [10]$$

From Eq. [9], the orientation factor Ω_B of the bicrystal can be described as

$$\Omega_B = \left(\frac{V_{G1}}{\Omega_{G1}} + \frac{V_{G2}}{\Omega_{G2}} \right)^{-1} \qquad [11]$$

B. *The Effect of Grain Boundary on the Cyclic Deformation*

The effect of GBs on the flow stresses was extensively discussed for bicrystals with GBs parallel to the stress axis. Chuang and Margolin[13] have given a stress relation for isoaxial β-brass bicrystals as

$$\sigma_T = \sigma_B + V_{GB} (\sigma_{GB} - \sigma_B) \qquad [12]$$

Where σ_{GB} was defined as the average stress in the GBAZ. It can be determined from the applied stress (σ_T), the flow stress (σ_B) of the single crystal, and the volume fraction (V_{GB}) in the GBAZ. The increase in flow stress in the bicrystal is attributed to the existence of the GBAZ. Mirura and Saeki[16] and Mirura *et al.*[17] also found that the flow stresses of bicrystals were increased by the presence of $\Sigma 7$ and $\Sigma 21$ coincidence GBs.

As shown in Figures 7 and 8, there is also a GBAZ in the bicrystal RB subjected to cyclic deformation. However, no such GBAZ exists in the bicrystal CB. Apparently, the difference in saturation stresses between the bicrystals CB and RB can be attributed to the higher mean stress in the GBAZ. As the bicrystals were cyclically saturated, their axial saturation stresses (Figures 5(a) and (b)) will have a relation similar to Eq. [12], as

$$\sigma_{as}^{RB} = \sigma_{as}^{CB} + V_{GB} (\sigma_{as}^{GB} - \sigma_{as}^{CB}) \qquad [13]$$

and

$$\sigma_{as}^{CB} = \sigma_{as}^{G1} V_{G1} + \sigma_{as}^{G2} V_{G2} \qquad [14]$$

where σ_{as}^{G1}, σ_{as}^{G2}, σ_{as}^{CB}, σ_{as}^{RB}, and σ_{as}^{GB} are the axial saturation stresses in the component crystals G1 and G2, the bicrystals

Table III. The Stresses in the GBAZ

Strain Amplitude	0.1 Pct	0.15 Pct	0.2 Pct	0.25 Pct	0.3 Pct
$\Delta\sigma^{B}_{as}$ (MPa)	4.9	6.2	7.3	8.7	9.8
σ^{GB}_{as} (MPa)	184.6	177.3	174.1	171.5	168.5

CB and RB, and in the GBAZ, respectively; V_{G1}, V_{G2}, and V_{GB} are the volume fraction of the component crystals G1 and G2, and the GBAZ, respectively. Here, $V_{G1} = V_{G2} = 0.5$. As listed in Table I, the difference in axial saturation stresses between the bicrystals CB and RB can be simply calculated as

$$\Delta\sigma^{B}_{as} = \sigma^{RB}_{as} - \sigma^{CB}_{as} \qquad [15]$$

If $\Delta\sigma^{B}_{as}$ is attributed to the higher mean stress (σ^{GB}_{as}) in the GBAZ, by combining Eq. [13] through [15], the mean stress in the GBAZ can be expressed as

$$\sigma^{GB}_{as} = \frac{\sigma^{RB}_{as} - \sigma^{CB}_{as}}{V_{GB}} + \sigma^{CB}_{as}$$
$$= \frac{\Delta\sigma^{B}_{as}}{V_{GB}} + \sigma^{CB}_{as} \qquad [16]$$

The calculated results of $\Delta\sigma^{B}_{as}$ and σ^{GB}_{as} at different strain amplitudes are listed in Table III by using the data in Tables I and II. It can be seen that the mean stress in the GBAZ is much higher than the mean stresses of the bicrystals CB and RB (σ^{CB}_{as} and σ^{RB}_{as}, respectively). From Eq. [16] and the results in Table III, it can be concluded that the increase in saturation stress and the disappearance of the plateau region in the CSSC of the bicrystal RB should be attributed to the higher stress in the GBAZ.

V. CONCLUSIONS

The cyclic deformation behavior of the copper bicrystals CB and RB and their component crystals, G1 and G2, was investigated and compared under constant total strain amplitude control. The following conclusions can be drawn.
1. The cyclic hardening rates and the axial saturation stresses increase, in order, in the component crystal G2, the bicrystal CB, the bicrystal RB, and the component crystal G1. By comparing the CSSCs of the component crystals and the bicrystals, it is found that the CSSCs of the component crystals and the bicrystal CB also show a plateau region at the measured strain range. However, the bicrystal RB does not display a plateau in its CSSC and has a higher saturation stress than the bicrystal CB.
2. Surface observations reveal that only the primary slip systems were activated within the component crystals for the bicrystal CB under the selected strain amplitudes. However, an additional slip system, A3, was observed in the vicinity of the GB in the bicrystal RB. The region

with the additional slip increases with strain amplitude and varies in the range from 265 to 650 μm.
3. In order to compare the cyclic deformation behavior of the copper bicrystals and their component crystals, an "orientation factor" for the bicrystal with a GB parallel to the stress axis was introduced. The cyclic saturation resolved shear stresses of the component crystals and the bicrystal CB nearly maintain the same value, in the range from 29 to 31 MPa. However, the saturation resolved shear stress of the bicrystal RB is increased from 31.4 to 34 MPa, which is higher than that of the bicrystal CB. Based on these results the effect of the GB on the cyclic deformation of the bicrystal RB was quantified.

REFERENCES

1. H. Mughrabi: *Mater. Sci. Eng.*, 1978, vol. 33, pp. 207-23.
2. Z.S. Basinski and S.J. Basinski: *Progr. Mater. Sci.*, 1989, vol. 36, pp. 89-48.
3. A.S. Cheng and C. Laird: *Mater. Sci. Eng.*, 1981, vol. 51, pp. 111-21.
4. S.P. Bhat and C. Laird: *Scripta Metall.*, 1978, vol. 12, pp. 687-92.
5. K.V. Rasmussen and O.B. Pedersen: *Acta Metall.*, 1980, vol. 28, pp. 1467-78.
6. O.B. Pedersen and K.V. Rasmussen: *Acta Metall.*, 1982, vol. 30, pp. 57-62.
7. V.-J. Kuokkala, T. Lepisto, and P. Kettunen: *Scripta Metall.*, 1982, vol. 16, pp. 1149-52.
8. H. Mughrabi: *Scripta Metall.*, 1979, vol. 13, pp. 479-83.
9. P. Lukas and L. Kunz: *Mater. Sci. Eng.*, 1985, vol. 74, pp. L1-5.
10. P. Lukas and L. Kunz: *Mater. Sci. Eng.*, 1994, vol. 189A, pp. L1-7.
11. Z. Yao and R.H. Wagoner: *Acta Metall. Mater.*, 1993, vol. 41, pp. 451-68.
12. J.P. Hirth: *Metall. Trans.*, 1972, vol. 3, pp. 3047-67.
13. Y.-D. Chuang and H. Margolin: *Metall. Trans.*, 1973, vol. 4, pp. 1905-17.
14. C. Rey and A. Zaoui: *Acta Metall.*, 1980, vol. 28, pp. 687-97.
15. C. Rey and A. Zaoui: *Acta Metall.*, 1982, vol. 30, pp. 523-35.
16. S. Mirura and Y. Saeki: *Acta Metall.*, 1978, vol. 26, pp. 93-101.
17. S. Mirura, K. Hamashima, and K.T. Aust: *Acta Metall.*, 1980, vol. 28, pp. 1591-1602.
18. H. Kawazoe, T. Takasugi, and O. Izumi: *Acta Metall.*, 1989, vol. 57, pp. 2883-94.
19. C.S. Li and T. Bretheau: *Acta Metall.*, 1989, vol. 37, pp. 2645-50.
20. X.L. Tan, H.C. Gu, and Z.G. Wang: *Mater. Sci. Eng.*, 1995, vol. 196A, pp. 45-52.
21. P. Sittner, V. Novak, and J. Bradler: *Scripta Metall. Mater.*, 1992, vol. 27, pp. 705-10.
22. P. Peralta and C. Laird: *Acta Mater.*, 1997, vol. 45, pp. 3029-46.
23. Y.M. Hu, Z.G. Wang, and G.Y. Li: *Scripta Mater.*, 1996, vol. 34, pp. 331-36.
24. Y.M. Hu, Z.G. Wang, and G.Y. Li: *Mater. Sci. Eng.*, 1996, vol. 208A, pp. 260-269.
25. Y.M. Hu and Z.G. Wang: *Int. J. Fatigue*, 1997, vol. 19, pp. 59-65.
26. Y.M. Hu and Z.G. Wang: *Acta Mater.*, 1997, vol. 45, pp. 2655-70.